Biochimica et Biophysica Acta 1818 (2012) 1717–1725

Contents lists available at SciVerse ScienceDirect

Biochimica et Biophysica Acta

journal homepage: www.elsevier.com/locate/bbamem

Topology and lipid selectivity of pulmonary surfactant protein SP-B in membranes: Answers from fluorescence

Elisa J. Cabré [a], Luís M.S. Loura [b,c,*], Alexander Fedorov [d], Jesus Perez-Gil [a,**], Manuel Prieto [d]

[a] Dept. Bioquímica, Fac. Biología, Universidad Complutense, 28040 Madrid, Spain
[b] Faculdade de Farmácia, Universidade de Coimbra, 3000-548 Coimbra, Portugal
[c] Centro de Química de Coimbra, 3004-535 Coimbra, Portugal
[d] Centro de Química-Física Molecular, Instituto Superior Técnico, and IN-Instituto de Nanociências e Nanotecnologias, 1049-0001 Lisboa, Portugal

ARTICLE INFO

Article history:
Received 5 January 2012
Received in revised form 12 March 2012
Accepted 13 March 2012
Available online 20 March 2012

Keywords:
Protein–lipid interaction
Lipid annulus
Fluorescence spectroscopy
Membrane protein topology
FRET

ABSTRACT

Contradictory results have been reported with respect to the depth of penetration and the orientation of pulmonary surfactant protein SP-B in phospholipid membranes and its relative selectivity to interact with anionic over zwitterionic phospholipid species. In the present study we have re-evaluated lipid–protein interactions of SP-B by analysing Förster resonance energy transfer (FRET) efficiencies, obtained from time-resolved measurements, from the single tryptophan in SP-B to different fluorescently labelled phospholipids in matrix bilayers made of either pure phosphatidylcholine (POPC) or the full lipid extract obtained from purified surfactant. In the background of POPC membranes SP-B exhibits a certain level of selectivity for anionic fluorescent phospholipids over the corresponding zwitterionic analogues, but apparently no preference for phosphatidylglycerol over other anionic species such as phosphatidylserine. No selectivity was detected in membranes made of full surfactant lipids, indicating that specific lipid–protein binding sites could already be occupied by endogenous anionic phospholipids. Furthermore, we have analysed the fit of two different models of how SP-B could be orientated with respect to phospholipid membrane surfaces to the FRET data. The FRET results are consistent with topology models in which the protein has a superficial orientation, with no regions of exclusion by the protein to the access of phospholipids, both in POPC membranes and in membranes made of the whole surfactant lipid fraction. This discards a deep penetration of the protein into the core of bilayers and suggests that most hydrophobic segments of SP-B could participate in protein–protein instead of lipid–protein interactions.

1. Introduction

Mammalian lungs are physically protected by a lipid–protein complex, which is spread on the thin water layer covering the respiratory epithelium. This complex, known as pulmonary surfactant, reduces the surface tension of the air–liquid interface drastically, impeding collapse of the alveoli at the end of expiration [1,2]. Premature babies with immature lungs lacking surfactant often suffer from neonatal respiratory distress syndrome (NRDS), a pathology that is routinely treated nowadays by supplementation with exogenous surfactants [3]. Infants or adults can also suffer from other surfactant dysfunctions associated with acute lung injury, such as the acute respiratory distress syndrome (ARDS), in which surfactant action is inhibited by the presence of serum components and inflammatory mediators leaked into the alveolar spaces [4]. The development of therapies to treat these complex pathologies depends on the production of new clinical surfactant preparations in high enough quantities and that in addition exhibit a proper resistance to inhibition [5,6].

Pulmonary surfactant is composed of roughly 90% lipids and 8–10% of specific surfactant-associated proteins, termed SP-A, SP-B, SP-C and SP-D (in chronological order of discovery) [7]. The most abundant phospholipid species in surfactant is dipalmitoylphosphatidylcholine (DPPC), which is also the main surface active component [8,9]. However, it is clear that surfactant lipids are not able by themselves to rapidly reach the air–liquid interface as they are secreted by type II pneumocytes in order to form operative surface active films. The presence of the hydrophobic surfactant proteins SP-B and SP-C is strictly required to facilitate an efficient transfer of phospholipids from surfactant stores (in the form of bilayers) at the aqueous hypophase into the interfacial film, and to maintain the film operative along the compression–expansion breathing cycles [10,11]. Most therapeutic surfactant preparations currently in use are obtained from animal sources and contain variable amounts of SP-B and SP-C. However, the molecular mechanisms by which surfactant proteins participate in the assembly, transport, and reorganisation of surfactant lipids at the respiratory surface are still not well understood.

* Corresponding author at: Faculdade de Farmácia, Universidade de Coimbra, Pólo das Ciências da Saúde, Azinhaga de Santa Comba, 3000-548 Coimbra, Portugal. Tel.: +351 239488485; fax: +351 239827126.
** Corresponding author. Dept. Bioquimica, Fac. Biologia, Universidad Complutense, Jose Antonio Novais 2, 28040 Madrid, Spain. Tel.: +34 91 3944994; fax: +34 91 3944672.
E-mail addresses: lloura@ff.uc.pt (L.M.S. Loura), jpg@bbm1.ucm.es (J. Perez-Gil).

0005-2736/$ – see front matter © 2012 Elsevier B.V. All rights reserved.
doi:10.1016/j.bbamem.2012.03.008

SP-B is essential from the very first inspiration at birth [12]. Lack of SP-B causes lethal respiratory failure in humans, as well as in SP-B-deficient genetically modified mice [13–15]. Absence of SP-B is accompanied by an incomplete processing of the SP-C precursor in alveolar air spaces [16,17] indicating that SP-B is somehow involved in the proper processing and assembly of the other hydrophobic surfactant protein. Mature SP-B is a 79-residue polypeptide, which derives from the proteolytic maturation of a longer precursor of 381 amino acids (42 kDa) produced in type II cells. SP-B processing is coupled to the assembly of surfactant membranes into lamellar bodies, the specific surfactant-storing organelles in pneumocytes. In the native form, SP-B contains intramolecular and intermolecular disulphide bonds stabilising a homodimeric structure [18]. The three-dimensional structure of SP-B has not yet been determined. Indirect measurements using spectroscopic techniques have revealed that the protein has an α-helical content of about 45%, probably in the form of amphipathic helical segments [19,20] and that it has limited conformational flexibility in different environments [20,21]. Sequence comparison and particularly the number and position of disulphides have lead to the inclusion of SP-B in the family of saposin-like proteins (SAPLIP) [22], together with saposins, NK-lysin and amoebapore. Saposin-like proteins seem to possess a membrane-free soluble conformation, which has been characterised at high resolution in several cases [23–25]. These homologies permitted to propose a structural model for SP-B based on the NMR structure of monomeric NK-lysin [26].

The essential role of SP-B in surfactant has been linked to the ability of the protein to promote a rapid transfer of phospholipids into air–water interfaces. SP-B, therefore, could be required to establish an operative surface active film from the earliest air–liquid respiratory interface. SP-B has been described to promote relatively large perturbations in membranes leading to lipid exchange and eventual fusion between liposome membranes and rapid leakage of their content [27–29]. Destabilisation of lipid packing in surfactant membranes could be part of the mechanism by which SP-B initiates exchange of phospholipids between surfactant membranes and the interfacial film. As a matter of fact, it has been proposed that hydrophobic surfactant proteins stabilise transition intermediates involved in interfacial adsorption [30]. A recent study proposes that the amphipathic character of SP-B, and particularly the high affinity for polar/non-polar interfaces of the region of the protein where its single tryptophan is located, could be important for inserting surfactant rapidly enough into the interface, during the brief periods of expansion at inspiration [31].

The elucidation of the mode and extent of interaction of SP-B with surfactant membranes and films is therefore important to fully understand its structure–function relationships. The detailed location and orientation of SP-B in phospholipid membranes as reconstituted in vitro have been a matter of controversy. On the one hand, evidence suggests that SP-B is located in a superficial region of membranes, with the polar positively-charged sides of the helical segments interacting with anionic phosphatidylglycerol (PG) and that superficial lipid–protein interaction would produce few perturbations on the acyl chain packing of surfactant phospholipids [32–34]. In contrast, other experiments have reported significant effects of SP-B on acyl chain order, consistent with a deeper penetration of SP-B in membranes and a direct perturbation by the protein of their hydrophobic core [35–37]. On the other hand, the extent of perturbation by SP-B of the structure and thermotropic properties of phospholipid membranes was shown to be critically dependent on the method used to reconstitute the lipid–protein complexes [38].

The occurrence of selective interactions between SP-B and anionic phospholipids in surfactant, such as phosphatidylglycerol (PG) has also been a matter of discussion. Inclusion of different phospholipid spin probes in membranes has allowed to determine that SP-B shows a preferential interaction with PG in membranes, compared to other zwitterionic or anionic species, as analysed by electron spin resonance (ESR) spectroscopy [35,39]. Other studies, however, have suggested that SP-B may prefer to partition into DPPC-enriched rather than DPPG-enriched regions in interfacial films, as detected by TOF-SIMS analysis of lipid–protein films transferred onto solid supports [40,41]. Although the time- and space-resolution of the information provided by spectroscopic and microscopic techniques could inform about very different SP-B/lipid processes [42], it has been argued that experimental detection of lipid–protein interactions might be impeded by the reconstitution of complexes at much higher protein proportions than those really existing in pulmonary surfactant membranes.

The single tryptophan (W9) in the sequence of mature SP-B is a unique tool to report information about the interactions and about the location and orientation of the protein within surfactant membranes by means of fluorescence spectroscopy. This tryptophan is part of a protein motif which is particularly important for the surface active function of SP-B [43], suggesting that particular interactions and structural features probed by W9 are of functional relevance. On the other hand, sensitivity and reliability of tryptophan fluorescence allow studying the behaviour of the protein in surfactant environments at lipid–protein ratios close to physiological conditions. This technique has been therefore used to obtain some information about the location of SP-B when interacting with phospholipid membranes and about possible occurrence of interactions between SP-B and the other hydrophobic protein in surfactant, SP-C [38,44].

In the present work, tryptophan fluorescence spectroscopy has been used both under steady-state and time-resolved regimes, to get further insight on the location, orientation and structural dynamics of SP-B in different membrane environments. Also, the existence of possible selective interactions between SP-B and particular phospholipid species has been explored again, now by analysing the occurrence of Förster resonance energy transfer (FRET) processes between SP-B tryptophan and 7-nitro-2-1,3-benzoxadiazol-4-yl (NBD)-labelled phospholipid probes included in the membranes. The sensitivity of FRET is particularly useful to retrieve information on the relative distribution of proteins and lipids in the range over which protein–lipid selectivity occurs. The existing models for quantification of protein–lipid selectivity by FRET, reviewed recently [45], apply to the situation of a transmembrane protein surrounded by an annular lipid region. In this work, a new model is derived for the important case of preferential interaction of a surface-located protein with lipid species lying directly underneath, which allowed us to establish this peripheral conformation as that adopted by SP-B in the studied systems.

2. Materials and methods

2.1. Materials

Chloroform and methanol were HPLC grade solvents from Scharlau (Barcelona, Spain). Sephadex LH-20 and LH-60 chromatography gels were obtained from Pharmacia, now GE Healthcare (Uppsala, Sweden). 1-Palmitoyl-2-oleoyl-*sn*-glycero-3-phosphocholine (POPC) and 1-oleoyl, 2-[12-[(7-nitro-2-1,3-benzoxadiazol-4-yl)amino]dodecanoyl]-PC, -PG and -PS (NBD-PC, NBD-PG and NBD-PS, respectively) were from Avanti Polar Lipids (Birmingham, AL, USA).

2.2. Isolation of SP-B and surfactant lipids

Surfactant protein SP-B was purified from porcine lungs as described elsewhere [21]. The purity of protein fractions was routinely checked by electrophoresis in SDS-polyacrylamide gels and quantified by amino acid analysis. The protein-depleted lipid fraction of purified pulmonary surfactant was obtained by chromatography in LH-20 of surfactant organic extract [46]. Lipid concentration was determined by phosphorus quantification [47].

2.3. SP-B reconstitution in phospholipid membranes

SP-B was reconstituted in POPC and the adequate labelled phospholipids to a final lipid concentration of ca. 1 mM, at a protein/lipid ratio of ~0.007. Concentration of NBD lipids ranged from 0 μM to 22 μM (0–2.2 mol%). Multilamellar lipid and lipid–protein suspensions (MLVs) were produced as follows. The appropriated amounts of NBD-labelled lipids, non-labelled lipids and protein were mixed in chloroform/methanol (2:1, v/v). Afterwards, the organic solvent was evaporated under a stream of dry nitrogen and last traces were removed by further evaporation under vacuum. Dried lipid or SP-B/lipid films were then resuspended in 50 mM Hepes buffer, pH 7.0 and MLVs were made by five freeze–thaw cycles with vortexing between each cycle. Vesicles were stored overnight at 4 °C until the experiment was performed. Final concentrations of unlabelled lipid and NBD lipids were assessed by phosphorus analysis [47] and the maximal UV–vis absorption ($\varepsilon_{max}(465\ nm) = 20{,}000\ M^{-1}\ cm^{-1}$), respectively.

2.4. Fluorescence spectroscopy

Steady-state fluorescence measurements were performed with an SLM Aminco 8100 Series 2 spectrofluorimeter (Rochester, NY; with double excitation and emission monochromators, MC400) in a right-angle geometry. The light source was a 450-W Xe arc lamp and for reference a Rhodamine B quantum counter solution was used. All measurements were performed at room temperature in 5×5 mm quartz cuvettes. Fluorescence decay measurements were carried out with a time-correlated single-photon timing system, which is described elsewhere [48]. Measurements were performed at room temperature. Excitation and emission wavelengths were 295 and 330 nm, respectively. Data analysis was carried out using a nonlinear, least-squares iterative convolution method based on the Marquardt algorithm [49]. The goodness of fit was judged from the experimental χ^2 value, weighted residuals, and autocorrelation plot. The decays are complex and described by a sum of three exponentials. The lifetime-weighted quantum yields of the donor in the presence and absence of acceptor (see Eq. 1) were determined upon analytical integration of the fitted curves.

3. Results

3.1. Lipid selectivity of SP-B

FRET is a photophysical phenomenon upon which the excitation of a molecule, the donor, is transferred to another, the acceptor. Energy transfer occurs over distances comparable to the dimensions of biological macromolecules. Due to the FRET process, the donor fluorescence is quenched, and the acceptor becomes excited. The FRET efficiency, E, can be obtained experimentally from the decrease of fluorescence intensity (I_{DA}) or lifetime ($\overline{\tau}_{DA}$) in the presence of increasing amount of acceptor, relative to their values in the absence of acceptor (I_D and $\overline{\tau}_D$, respectively):

$$E = 1-\overline{\tau}_{DA}/\overline{\tau}_D = 1-I_{DA}/I_D. \quad (1)$$

The experimental FRET efficiency between a chosen donor and acceptor can report on lipid–protein interaction. In the present study, FRET was performed to gain insight into SP-B topology in membranes and used to analyse qualitatively and quantitatively the selectivity of the protein for different fluorescently-labelled phospholipids. These studies were carried out upon reconstitution of SP-B in POPC, using the single tryptophan of the protein as a donor for FRET to small fractions of PC (phosphatidylcholine), PG (phosphatidylglycerol) or PS (phosphatidylserine) derivatised with NBD in the *sn*-2 acyl chain, as acceptors. High FRET efficiencies between SP-B tryptophan (donor) and certain NBD-lipids (acceptors) would point to selectivity because that would indicate that those phospholipids have higher probability of location near the protein vicinity. Conversely, low FRET efficiencies would mean that there is no preference for a given lipid species, but instead a random distribution of the phospholipid probes in the membrane matrix where the protein is embedded, with no enrichment near the protein.

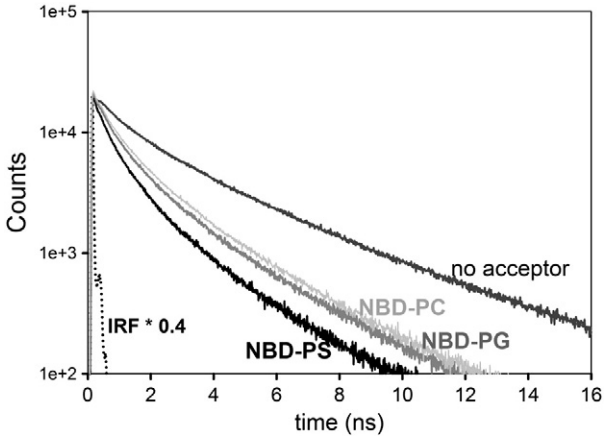

Fig. 1. Decays of the fluorescence of SP-B tryptophan in the absence and in the presence of FRET acceptors (NBD-lipids) in a POPC membrane matrix.Acceptor concentration: ~2.5 mol% (corresponding to the last point of each series in Fig. 2), 0 mM NaCl. IRF denotes the instrumental response function (laser excitation profile), and is multiplied in the plot by a 0.4 factor for the sole sake of representation.

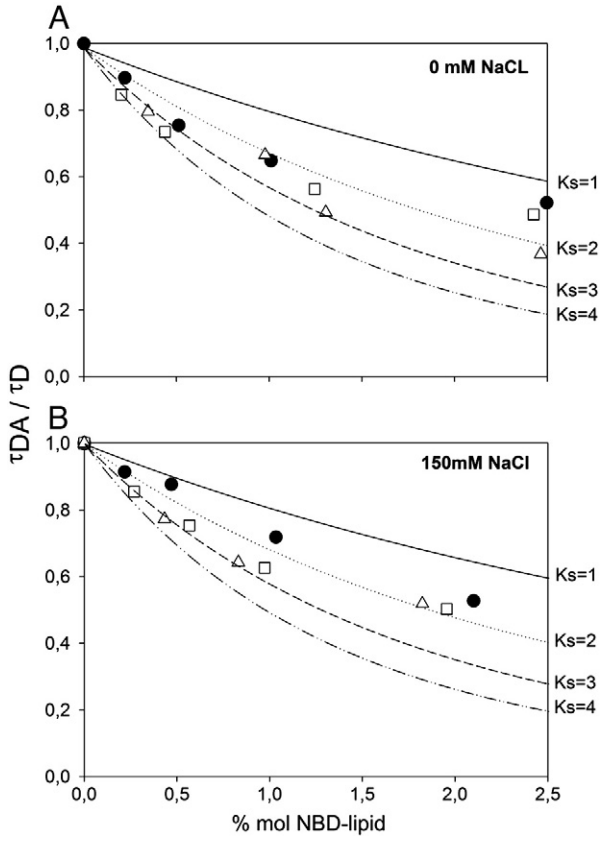

Fig. 2. Donor (SP-B tryptophan) fluorescence quenching by FRET acceptor (NBD-lipids) in a POPC membrane matrix.Experimental time-resolved FRET data have been obtained in 50 mM Hepes buffer, pH 7.0, at low (0 mM NaCl, panel A) or physiological (150 mM NaCl, panel B) ionic strength. Acceptors were NBD-PC (closed circles), NBD-PG (squares) or NBD-PS (triangles). Lines are the theoretical curves for the different indicated selectivity constant K_s values, which consider the topology of the protein in the membrane.

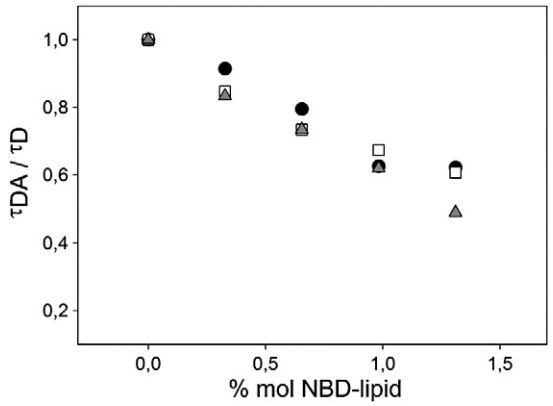

Fig. 3. Donor (SP-B tryptophan) fluorescence quenching by FRET acceptor (NBD-lipids) in a membrane matrix reconstituted from the whole surfactant lipid fraction.Symbols, as indicated in Fig. 1, are the experimental data obtained at low ionic strength in 50 mM Hepes buffer, pH 7.0.

The experimental FRET efficiencies were obtained in these experiments from the measured quenching of donor fluorescence (Eq. 1), in 50 mM Hepes buffer, pH 7.0, in the absence of salt or in the presence of 150 mM NaCl. Fig. 1 shows typical SP-B fluorescence decays used to calculate FRET efficiencies using Eq. 1. Fig. 2A illustrates how at low salt content FRET from SP-B tryptophan is less efficient towards zwitterionic NBD-PC than to the negatively charged species NBD-PG or NBD-PS. No significant differences in FRET efficiency between the latter two acceptor species could be detected. The only data point for which FRET to NBD-PG is noticeably less efficient than to NBD-PS is that of the sample with the highest NBD-lipid concentration. For the other points, especially those with lower acceptor concentration (less susceptible to potential probe perturbing effects), FRET efficiency to NBD-PG is clearly higher than to NBD-PC, and generally comparable with that to NBD-PS. At physiological ionic strength (Fig. 2B), similar trends are observed. In contrast to the data previously reported using spin-labelled lipids [35], significant differences in selectivity between PG and PS could not be detected. The experimental data obtained for FRET from SP-B to NBD-labelled lipids have been compared in Fig. 2 with the theoretical behaviour expected considering a random distribution of donor and acceptor probes in the membranes (dashed line in Fig. 2 for a selectivity constant $K_s = 1$, calculations were done as described in the Appendix A). These theoretical calculations require modelling the expected topology of the protein in the membranes, as well as the expected nature of lipid–protein interaction (see next section).

Selectivity experiments were also performed in host membranes reconstituted from the full lipid extract of native surfactant, at low ionic strength and pH 7.0. The efficiency of FRET from the protein to the different acceptors in these membranes is shown in Fig. 3. No clear trend was observed with respect to a particularly higher FRET efficiency towards certain lipid species that could be indicative of some degree of selectivity. Considering that the whole lipid fraction obtained from surfactant already contains in the order of 10–15% by mass of anionic phospholipids, one can assume that the potentially specific lipid-binding sites in SP-B are already occupied by endogenous PG or PI in these compositionally native-like membranes.

3.2. SP-B topology in membrane

The FRET experiments carried out to analyse the potential selectivity of SP-B for interaction with certain phospholipid species also provided valuable information on SP-B topology in the membranes. In particular, the experimentally measured FRET efficiency between the protein donor and the lipid acceptors and its dependence on the density of acceptors depends critically on the geometry and stoichiometry of the lipid–protein interaction. The experimental data can thus be compared with the theoretical expectations according to different topological models and one can evaluate which of them provides a better match to the experimental behaviour. The FRET efficiencies obtained towards labelled zwitterionic phospholipids (NBD-PC), for which no selectivity is expected, are particularly useful in this respect.

Two different theoretical models could describe the two main possible protein arrangements in the membrane (see Fig. 4). The starting point to apply the models was to establish the projection of the SP-B molecule over the membrane in order to estimate the number of phospholipid molecules that would be in direct contact with SP-B. This calculation was made by modelling the three dimensional structure of the monomer of porcine SP-B using the crystal structure of the human saposin-C (PDB ID: 2GTG) as a template [50,51]. The face of the protein that interacts with the membrane was arbitrarily defined as the one that maximises interaction. The total area calculated for the interaction of the protein monomer on the membrane plane was 989 Å^2, which

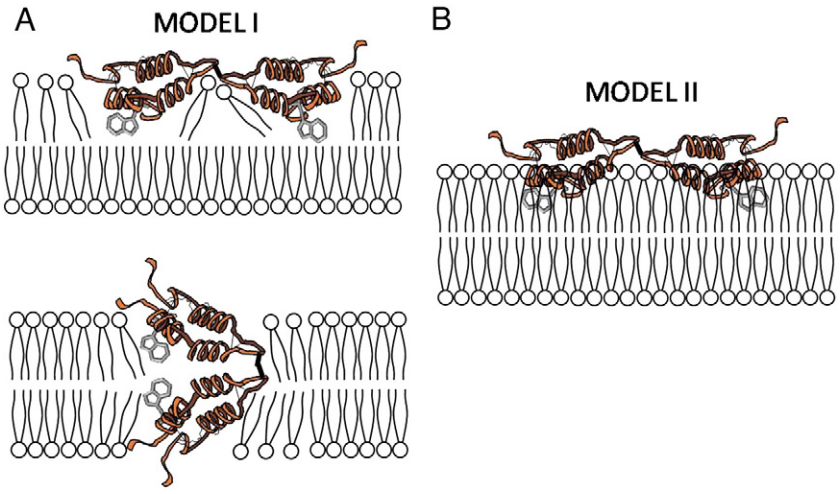

Fig. 4. Theoretical molecular models for the topology of SP-B in phospholipid membranes.Panel A represents model I, where the protein insertion leads to a volume exclusion in the membrane occupied by the protein instead of lipids (and therefore represents an exclusion area for FRET acceptors). Panel B represents model II, where the protein exhibits a superficial interaction with the membrane surface, with no lateral lipid excluded area. Single FRET donors (Trp residues) per SP-B monomer are indicated.

covers around 14 lipid molecules per monomer. The stoichiometry of SP-B/lipid interactions, determined experimentally by techniques such as calorimetry [52] or ESR [35], is significantly larger, in the order of 35–50 lipid molecules perturbed per monomer of SP-B, but this refers to the number of lipid molecules that sense the presence of protein, while the stoichiometry numbers used in the present study refer to lipid molecules directly in touch with the protein in the range of distance defined by the Trp/NBD FRET, which Förster distance (R_0) value, determined by us in this study, is 22 Å (see Appendix A). The defined geometry of SP-B protein for developing the models used here is a flat cylinder with the single tryptophan residue placed in the geometrical centre.

Fig. 4 represents schematically how SP-B can be embedded in the membrane in two different ways: In model 1, a deep embedment of the protein in the membrane would create an area of exclusion of phospholipid molecules equivalent to the surface taken up by the protein. A topologically equivalent situation would occur if the protein dimer would span the whole bilayer thickness, as proposed in certain models [26]. Donor quenching by FRET in this first model could arise from two distinct acceptor populations: one located in a single circular layer of annular lipid surrounding the protein, and another uniformly distributed beyond the annular region. The formalism for this molecular arrangement was recently described by us (see [53] for a detailed derivation) and is readily adaptable to the present case. The main difference resides on the number of molecular sites in the annular region. In the published work, the donor protein consisted of a single transmembrane helix, and 12 annular sites were postulated, 6 per leaflet (see Eq. 10 of [53]). In the present study, a protein monomer radius of 18 Å was estimated from the projected area value mentioned above, consistent with 12 molecules in the annular region in each leaflet. It was verified that the theoretical efficiency obtained with this formalism is very low when compared to the experimental measurements for reasonable values of the model parameters (not shown). Consideration of the eventuality of protein dimerisation would still reduce the theoretical efficiency even further, due to the increased exclusion distance. For this reason, this model was discarded in the quantitative analysis of lipid selectivity.

This led us to consider a second model, schematically depicted in Fig. 4B, which assumes that the protein adsorbs to the membrane surface. FRET can again occur to two distinct acceptor populations, one located directly below the protein (where the possibility of acceptor enrichment due to protein–lipid selectivity is considered) and another, located beyond this region (bulk bilayer). This model, which is described in detail in Appendix A, is compatible with the high experimental FRET efficiencies measured, because (i) since the protein sits on top of the bilayer, there is no lateral exclusion distance, and acceptors can potentially locate directly below the donor protein, and (ii) because the fluorophore of an acyl chain-labelled NBD probe does not sit in the interior of the bilayer but loops to the surface instead [54,55], the transverse exclusion distance w (see Appendix A) is expected to be small. As shown in Fig. 2A and B, the selectivity parameter $K_s = 1$ plots still predict less FRET efficiency than measured experimentally, even for the zwitterionic probe NBD-PC, and some degree of probe preference must be invoked (the experimental data are in fact closer to the $K_s = 2$ curves). This could in principle result from inadequate choice of some model parameters (variables which are involved in the model include the hypothetical cylindrical protein homodimer radius R_p, the transverse distance between the donor and acceptor planes w, area/lipid (for calculation of surface concentration) and R_0 (and all parameters that in turn are required for its calculation: donor quantum yield, acceptor molar absorptivity, refractive index of the medium and orientation factor)). However, it is noteworthy that this type of behaviour was previously observed in the annular lipid distribution around M13 major coat protein (for which $K_s = 2.0$ was determined for a NBD-PC in a DOPC matrix, and higher values, of up to $K_s = 3.0$, were determined for anionic NBD lipids), and may be caused by favourable interaction of the NBD fluorophore with suitable protein residues. It was shown that the O atoms of the nitro group of the NBD fluorophore, which have partial charges near −0.5, are deeply involved as H-bond acceptors to water molecules in fluid DPPC bilayers [54]. Similarly, these NBD atoms may be involved in electrostatic or H-bonding interactions with suitable positively charged and/or H-bond donor SP-B atoms. This would probably lead to a higher occupation of the lipid sites below each protein molecule than predicted on the basis of a strictly uniform distribution, hence the recovered K_s value. Bearing this in mind, one can conclude that our results support the view that SP-B, in agreement with other reported studies [32,33,56], lies on the membrane surface, with its α-helical segments orientated more or less parallel to the bilayer plane [34] as schematised in Fig. 4B. Anionic phospholipids, for which higher FRET efficiencies were observed (as commented above), are enriched in the bilayer region below the protein, with K_s in the range of 2–4.

FRET curves obtained in membranes prepared from the full lipid fraction of surfactant also showed a qualitatively similar dependence on the density of acceptors as observed in purely zwitterionic membranes, although with no apparent selectivity for anionic phospholipid probes, as described above. This indicates that SP-B also adopts this superficial orientation in native-like membranes containing a fair proportion of anionic phospholipids.

4. Discussion

Previous studies, using different technical approaches, have dealt with the orientation of SP-B in membranes, which has been a matter of controversy. On the one hand, several pieces of evidence suggested that SP-B is located in a superficial region of membranes, producing little perturbations on the acyl chain packing of surfactant phospholipids [32–34]. Other experiments, in contrast, have reported significant effects of SP-B on acyl chain order, consistent with a deeper penetration of SP-B in membranes and a direct perturbation by the protein of their hydrophobic core [35–37]. Interestingly, the extent of perturbation by SP-B on the structure and thermotropic properties of phospholipid membranes was found to be critically dependent on the method used to reconstitute the lipid–protein complexes [38,57].

The fluorescence of the single tryptophan of SP-B has been previously used to obtain information about the location of SP-B when interacting with phospholipid membranes, and it was found that the tryptophan of the protein always adopts a superficial location at the surface of the membranes [38]. However, the strict situation of the tryptophan residue does not tell very much about the orientation of the protein as a whole, because very often membrane proteins with either peripheral or integral insertion locate their aromatic side chains close to the headgroup region of the membrane [58]. In the present study, information on the topology of SP-B has not been obtained directly from the fluorescence of the single Trp in the protein but from the occurrence of FRET from SP-B Trp to a phospholipid acceptor probe, whose accessibility depends on the structure and orientation of the whole protein. Previous steady state fluorescence assays reported only qualitative behaviour of the SP-B protein [20,21,38]. The present work gives the first reliable quantitative analysis of the interaction of SP-B with lipid membranes due, specifically, to the use of time-resolved fluorescence, which is a powerful tool that overcomes the inherent light scatter of multilamellar vesicles, which interfere substantially with steady state fluorescence measurements.

The topology of the interaction of surfactant protein SP-B with lipid membranes is not understood in detail, and several different predictions of the location of SP-B in a phospholipid environment have been proposed [7,31]. In the present study we have analysed

two different potential models of how SP-B could be orientated with respect to phospholipid membrane surfaces, and determined whether FRET efficiencies obtained from time-resolved measurements are consistent with any of the topology models. Model I is derived for an integrated protein in the membrane, but could be applied to certain topologies proposed for the covalent dimer of SP-B, in which the protein dimerisation interface would be in the inner hydrophobic core of the bilayer, and the flanking positively charged residues would be exposed on each side of the bilayer [26]. Although the occurrence of such a topology would be difficult to explain in native surfactant membranes, considering the way SP-B is originated from the maturation and interaction with membranes of the SP-B precursor [59], the reconstitution of SP-B/lipid complexes in vitro, from lipid–protein mixtures in organic solvent, could well force the exposure to the hydrophobic core of membranes of hydrophobic segments that would be shielded from the membrane contact in other conformations. With this orientation of the SP-B dimer in the membrane, the tryptophans of the protein would be still located at the headgroup region of the bilayer, close to the surface of the membranes, as determined experimentally [38]. This theoretical transmembrane-like disposition of the protein would cause an extensive perturbing effect on membrane packing, as previously reported [35–37]. Such orientation would be also compatible with the interaction of SP-B with the inner core of bilayers at the edges of membrane discs, a type of membrane structure that has been proposed as promoted by the protein [60,61]. The calculations made in the present study used dimensional parameters similar to those defined by the model of Zaltash and co-workers [26]. In that structural model, the diameter calculated for each SP-B monomer is 37 Å (we estimated 35.4 Å), and its projected area on the bilayer is similar to our value of 989 $Å^2$. According to this model I, SP-B would be integrated in membranes in a similar manner to that of an integral transmembrane protein, surrounded by an annular shell of lipids in direct contact with the protein (Fig. 4A). However, when the theoretical expectation of FRET from Trp to NBD-PC according to model I was compared with the experimental data, it was found that experimental efficiency rates were much higher than expected according to the model (not shown). Experimental data would also discard other similar topological models that would imply the existence of a region of lipids topologically excluded from the protein.

This deviation led us to consider a different topology, in which SP-B is assumed to be a strictly superficial protein, as defined by model II in Fig. 4. The new topology proposed was intended to account for higher experimental FRET efficiencies, through a higher number of lipid molecules potentially interacting per protein molecule. To this effect, a new FRET model accounting for the preferential interaction of a surface-located protein with lipid species lying directly below it was derived. The new theoretical curve derived from this model was compared with the experimental FRET efficiencies, and an adequate description was obtained. It is therefore concluded that SP-B, in agreement with other reported studies [32,33,62], lies on the membrane surface, with its α-helical segments somehow orientated in a parallel manner to the bilayer surface [34], and with the protein potentially interacting with phospholipid headgroups. This superficial location of SP-B also agrees with the observed degree of insertion of SP-B in the membrane as described in a previous work [38], including the location of the single tryptophan of SP-B in the membranes, determined by the fluorescence quenching parallax method, and limited perturbation by the protein of the phospholipid acyl chains. The topological organisation of SP-B with respect to the phospholipid environments would be maintained in synthetic SP-B analogues, which can supposedly mimic some aspects of full-length SP-B activity, such as is the case for a synthetic peptide segment containing the N-terminal 25 amino acids of SP-B ($SP\text{-}B_{1-25}$) [63]. Detailed topographical mapping of $SP\text{-}B_{1-25}$ in different membranes has been approached [64], which is consistent with the parallel and superficial resting of this segment of SP-B over the membrane.

The study of lipid selectivity with the FRET technique made it possible to detect in a semi-quantitative way that SP-B shows certain selectivity towards interaction with anionic phospholipids, with negligible differences in specificity between different anionic species. In a previous study, it was shown using electron spin resonance (ESR) that SP-B exhibits a certain selectivity for the anionic phosphatidylglycerol (PG) [35]. Preferential interaction of SP-B with PG headgroups in surfactant membranes was proposed earlier, with participation of the highly conserved positively charged amino acids of the protein [19,56]. Selection of the polyolic anionic lipids PG and PI in the context of SP-B/lipid interactions should be based on more than only electrostatic interactions, possibly including complex interactions at defined protein sites. The FRET results reported here do not allow us to detect any selectivity between different anionic phospholipidic species, but it is possible that the bulky fluorescent groups labelling the phospholipids could mask subtle interactions required for a more specific recognition. A similar behaviour was found in the context of membranes reconstituted from the whole surfactant lipid fraction obtained from pig lungs, the same source from which the protein was purified, discarding possible specific effects of minor lipid components in surfactant on the orientation and lipid selectivity of SP-B.

The putative in vivo orientation of SP-B in membranes should be interpreted with caution, because properties of SP-B as determined in vitro are likely to be strongly influenced by a number of variables in sample preparation. As a matter of fact, the way SP-B disturbs the host bilayers has been reported to depend critically on how the lipid–protein complexes are prepared [57]. We could expect SP-B to be more integrated into the membrane if the lipids and the protein are dried at the same time instead of adding SP-B to preformed vesicles, as in the latter case the protein could be preferentially interacting with the outer surface of the membrane. In this study, membranes were reconstituted by simultaneously co-drying and re-hydrating protein and lipids. Significantly, we concluded that, even using this procedure, SP-B was found to interact with the host membrane in a superficial manner. The conclusion is therefore that the fundamental activity of SP-B to promote transfer of phospholipid molecules between surfactant membranes, or between lipid–protein complexes and the interface, is performed from a relatively peripheral location. This orientation is probably important to maximise the interactions that permit the protein to bridge membranes, or to connect surfactant membranes with the interface. SP-B-promoted inter-membrane connections are likely crucial to ensure a rapid flow of surface active lipid species all through the membrane network that saturates the alveolar surface [1,65]. Also, to facilitate a rapid diffusion of oxygen through the interface, without the limitation imposed by the poor solubility of oxygen into aqueous phases [66]. Recent data did in fact confirm that SP-B promotes formation of multilayer membrane arrays, mediated by a necessary establishment of protein–protein interactions [67]. The present results could indicate that a fair proportion of the highly hydrophobic segments of the protein are used to establish protein–protein interactions, which may mediate assembly of lipid-transferring supramolecular structures, and not that much to sustain a deep embedment of the protein into membranes. The elucidation of the structure and molecular mechanism of those potential SP-B-based protein assemblies, as well as the determination of the spatio-temporal framework of their interaction with surfactant membranes and films, will be essential to understand structure–function determinants in surfactant and to design more efficient therapeutic surfactant preparations in the future.

Acknowledgements

This research has been supported by grants from the Spanish Ministry of Science (BIO2009-09694, CSD2007-00010), Community of

Madrid (S0505/MAT/0283), and Complutense University (to EJC and JP-G). AF and MP acknowledge funding from Fundação para a Ciência e Tecnologia (Portugal), project references PTDC/QUI-BIQ/099947/2008 and PTDC/QUI-BIQ/112067/2009. LMSL acknowledges funding by FEDER, through the COMPETE program (FCT project FCOMP-01-0124-FEDER-010787 (FCT PTDC/QUI-QUI/098198/2008)).

Appendix A

Here we derive the equations used for the FRET calculations in the context of model II. Consider a cylindrical protein (radius R_p), with a donor fluorophore located at its axis, adsorbed to the surface of a lipid bilayer leaflet containing acceptors. Consider also that the protein covers N_{MAX} lipid molecules at the bilayer surface, each of which can be either non-labelled or labelled with NBD acceptor. For an overall fraction of NBD lipid $x_{NBD}<<1$ (as always verified in the experiment), the probability of one of the covered molecules being labelled is given by

$$\mu = K_S \frac{N_{NBD}}{N_L} = K_S x_{NBD} \tag{A1}$$

where N_{NBD} is the overall number of NBD-labelled lipid, N_L is the total overall number of lipid molecules, and K_s is the protein lipid selectivity (equal to 1, for no selectivity of the labelled lipids relative to the non-labelled species). Donors and acceptors in general have different transverse positions, residing in parallel planes separated by a distance w (Fig. 5).

We now use a probabilistic approach to the calculation of the FRET contribution of the acceptors below the protein, similar to the one described in [53] for annular acceptor distribution:

$$\rho_1(t) = \sum_{i=0}^{N_{MAX}} \binom{N_{MAX}}{i} \mu^i (1-\mu)^{N_{MAX}-i} \prod_{j=1}^{i} \exp\left(-k_{Tj} t\right) \tag{A2}$$

where

$$\binom{N_{MAX}}{i} = \frac{i!}{N_{MAX}!(N_{MAX}-i)!}. \tag{A3}$$

The product in the right-hand side is calculated using the dependence of k_{Tj} on the distance R_j between the donor and the jth acceptor, $k_{Tj} = (t/\tau_D)(R_0/R_j)^6$ (where R_0 is the Förster distance, and τ_D is the excited-state lifetime in the absence of FRET) and introducing a distance distribution function $W(R_j)$ to consider all statistical positions of acceptors [68,69]. Because all acceptors have the same statistical distribution, all $W(R_j)$ are identical, and one obtains

$$\prod_{j=1}^{i} \exp\left(-k_{Tj} t\right) = \prod_{j=1}^{i} \exp\left[-\frac{t}{\tau_D}\left(\frac{R_0}{R_j}\right)^6\right] = \prod_{j=1}^{i} \int_{w}^{\sqrt{w^2+R_p^2}} \exp\left[-\frac{t}{\tau_D}\left(\frac{R_0}{R_j}\right)^6\right] W\left(R_j\right) dR_j = [J(t)]^i \tag{A4}$$

where $J(t)$ denotes the integral term. Introducing a uniform $W(R)$ distribution and making the substitution $\alpha = \cos\theta$ (where θ is defined in Fig. 5), one arrives at the following expression for $J(t)$ [69]:

$$J(t) = \frac{2w^2}{R_p^2} \int_{w/\sqrt{w^2+R_p^2}}^{1} \exp\left[-\frac{t}{\tau_D}\left(\frac{R_0}{w}\right)^6 \alpha^6\right] \alpha^{-3} d\alpha. \tag{A5}$$

This function is calculated numerically for each t. It only depends on the values assumed for R_0, w and R_p (or the adimensional parameters R_p/R_0 and w/R_0).

Beyond the membrane region directly below the protein, the survival probability of the donor excited state (taking into account FRET to acceptors in this region), ρ_2, is given by [69]

$$\rho_2(t) = \exp\left\{-2n\pi w^2 \int_0^{w/\sqrt{w^2+R_p^2}} \frac{1-\exp\left(-tb^3\alpha^6\right)}{\alpha^3} d\alpha\right\} \tag{A6}$$

where $b = (R_0/w)^2$ and n is the density (molecules/unit area) of acceptors in the region under consideration. For dilute protein concentration, n is virtually identical to the overall acceptor density, n_0. Otherwise, n is calculated from

$$n = n_0 \frac{1-K_S(N_P/N_L)N_{MAX}}{1-(N_P/N_L)N_{MAX}} \tag{A7}$$

where N_P is the overall number of protein molecules.

The overall donor decay is obtained by multiplying the donor decay in absence of acceptor, $i_D(t)$, by the FRET terms $\rho_1(t)$ and $\rho_2(t)$:

$$i_{DA}(t) = i_D(t)\rho_1(t)\rho_2(t). \tag{A8}$$

The above equation applies to the case where FRET to the opposing bilayer leaflet is negligible. Otherwise, the product in Eq. A8 should include additional $\rho_1(t)$ and $\rho_2(t)$ terms. These are again calculated using Eqs. A1–A7, replacing only the value of the interplanar distance w. In our calculations, the relevant input parameters were $R_0 = 22$ Å (calculated from spectroscopic data, assuming Trp quantum yield 0.10, ε_{max}(NBD-lipid) = 20,000 M^{-1} cm^{-1}, refractive index 1.4 and orientation factor 2/3 (dynamic isotropic limit); see e.g. [48]), $w_1 = 2$ Å (FRET to the bilayer leaflet to which the protein is adsorbed), $w_2 = 24$ Å (FRET to the opposing leaflet, which could be neglected with very minor alterations) and $R_p = 25$ Å (estimated for a hypothetical cylindrical homodimer, with projected area double of that calculated for the monomer).

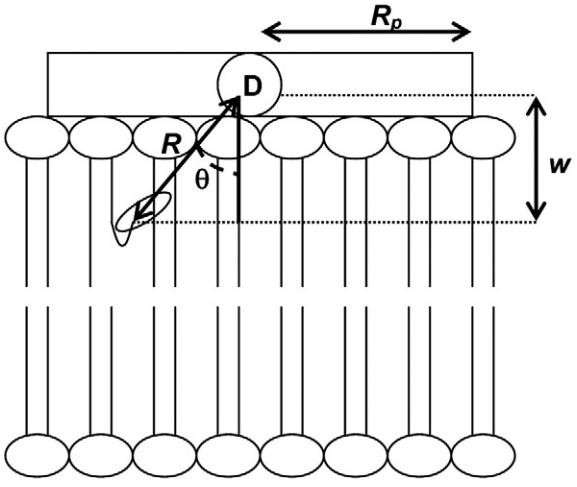

Fig. 5. Donor–acceptor geometrical parameters relevant to model II.

References

[1] J. Pérez-Gil, Structure of pulmonary surfactant membranes and films: the role of proteins and lipid–protein interactions, Biochim. Biophys. Acta 1778 (2008) 1676–1695.
[2] Y.Y. Zuo, R.A. Veldhuizen, A.W. Neumann, N.O. Petersen, F. Possmayer, Current perspectives in pulmonary surfactant—inhibition, enhancement and evaluation, Biochim. Biophys. Acta 1778 (2008) 1947–1977.
[3] J.D. Merrill, R.A. Ballard, Pulmonary surfactant for neonatal respiratory disorders, Curr. Opin. Pediatr. 15 (2003) 149–154.
[4] J.F. Lewis, R. Veldhuizen, The role of exogenous surfactant in the treatment of acute lung injury, Annu. Rev. Physiol. 65 (2003) 613–642.

[5] O. Blanco, J. Perez-Gil, Biochemical and pharmacological differences between preparations of exogenous natural surfactant used to treat Respiratory Distress Syndrome: role of the different components in an efficient pulmonary surfactant, Eur. J. Pharmacol. 568 (2007) 1–15.
[6] I. Mingarro, D. Lukovic, M. Vilar, J. Perez-Gil, Synthetic pulmonary surfactant preparations: new developments and future trends, Curr. Med. Chem. 15 (2008) 393–403.
[7] J. Johansson, T. Curstedt, Molecular structures and interactions of pulmonary surfactant components, Eur. J. Biochem. 244 (1997) 675–693.
[8] R.H. Notter, J.N. Finkelstein, Pulmonary surfactant: an interdisciplinary approach, J. Appl. Physiol. 57 (1984) 1613–1624.
[9] J.A. Clements, Functions of the alveolar lining, Am. Rev. Respir. Dis. 115 (1977) 67–71.
[10] J. Perez-Gil, K.M. Keough, Interfacial properties of surfactant proteins, Biochim. Biophys. Acta 1408 (1998) 203–217.
[11] J. Pérez-Gil, Lipid–protein interactions of hydrophobic proteins SP-B and SP-C in lung surfactant assembly and dynamics, Pediatr. Pathol. Mol. Med. 20 (2001) 445–469.
[12] J.A. Whitsett, L.M. Nogee, T.E. Weaver, A.D. Horowitz, Human surfactant protein B: structure, function, regulation, and genetic disease, Physiol. Rev. 75 (1995) 749–757.
[13] J.C. Clark, S.E. Wert, C.J. Bachurski, M.T. Stahlman, B.R. Stripp, T.E. Weaver, J.A. Whitsett, Targeted disruption of the surfactant protein B gene disrupts surfactant homeostasis, causing respiratory failure in newborn mice, Proc. Natl. Acad. Sci. U. S. A. 92 (1995) 7794–7798.
[14] K. Tokieda, J.A. Whitsett, J.C. Clark, T.E. Weaver, K. Ikeda, K.B. McConnell, A.H. Jobe, M. Ikegami, H.S. Iwamoto, Pulmonary dysfunction in neonatal SP-B-deficient mice, Am. J. Physiol. 273 (1997) L875–L882.
[15] J.M. Klein, M.W. Thompson, J.M. Snyder, T.N. George, J.A. Whitsett, E.F. Bell, P.B. McCray Jr., L.M. Nogee, Transient surfactant protein B deficiency in a term infant with severe respiratory failure, J. Pediatr. 132 (1998) 244–248.
[16] D.K. Vorbroker, S.A. Profitt, L.M. Nogee, J.A. Whitsett, Aberrant processing of surfactant protein C in hereditary SP-B deficiency, Am. J. Physiol. 268 (1995) L647–L656.
[17] T.E. Weaver, J.J. Conkright, Function of surfactant proteins B and C, Annu. Rev. Physiol. 63 (2001) 555–578.
[18] J. Johansson, T. Curstedt, H. Jornvall, Surfactant protein B: disulfide bridges, structural properties, and kringle similarities, Biochemistry 30 (1991) 6917–6921.
[19] M. Andersson, T. Curstedt, H. Jornvall, J. Johansson, An amphipathic helical motif common to tumourolytic polypeptide NK-lysin and pulmonary surfactant polypeptide SP-B, FEBS Lett. 362 (1995) 328–332.
[20] A. Cruz, C. Casals, J. Perez-Gil, Conformational flexibility of pulmonary surfactant proteins SP-B and SP-C, studied in aqueous organic solvents, Biochim. Biophys. Acta 1255 (1995) 68–76.
[21] J. Pérez-Gil, A. Cruz, C. Casals, Solubility of hydrophobic surfactant proteins in organic solvent/water mixtures. Structural studies on SP-B and SP-C in aqueous organic solvents and lipids, Biochim. Biophys. Acta 1168 (1993) 261–270.
[22] R.S. Munford, P.O. Sheppard, P.J. O'Hara, Saposin-like proteins (SAPLIP) carry out diverse functions on a common backbone structure, J. Lipid Res. 36 (1995) 1653–1663.
[23] V.E. Ahn, K.F. Faull, J.P. Whitelegge, A.L. Fluharty, G.G. Prive, Crystal structure of saposin B reveals a dimeric shell for lipid binding, Proc. Natl. Acad. Sci. U. S. A. 100 (2003) 38–43.
[24] O. Hecht, N.A. Van Nuland, K. Schleinkofer, A.J. Dingley, H. Bruhn, M. Leippe, J. Grotzinger, Solution structure of the pore-forming protein of *Entamoeba histolytica*, J. Biol. Chem. 279 (2004) 17834–17841.
[25] E. Liepinsh, M. Andersson, J.M. Ruysschaert, G. Otting, Saposin fold revealed by the NMR structure of NK-lysin, Nat. Struct. Biol. 4 (1997) 793–795.
[26] S. Zaltash, M. Palmblad, T. Curstedt, J. Johansson, B. Persson, Pulmonary surfactant protein B: a structural model and a functional analogue, Biochim. Biophys. Acta 1466 (2000) 179–186.
[27] L.A. Francis, R. Poulain, Mary C. Williams, Robert L. Hamilton, Samuel Hawgood, Effect of surfactants apolipoproteins on liposome structure: implications for tubular myelin formation, Am. J. Physiol. 262 (1992) L730–L739.
[28] M.A. Oosterlaken-Dijksterhuis, M. van Eijk, L.M. van Golde, H.P. Haagsman, Lipid mixing is mediated by the hydrophobic surfactant protein SP-B but not by SP-C, Biochim. Biophys. Acta 1110 (1992) 45–50.
[29] M.A. Ryan, X. Qi, A.G. Serrano, M. Ikegami, J. Perez-Gil, J. Johansson, T.E. Weaver, Mapping and analysis of the lytic and fusogenic domains of surfactant protein B, Biochemistry 44 (2005) 861–872.
[30] V. Schram, S.B. Hall, Thermodynamic effects of the hydrophobic surfactant proteins on the early adsorption of pulmonary surfactant, Biophys. J. 81 (2001) 1536–1546.
[31] A.G. Serrano, J. Perez-Gil, Protein–lipid interactions and surface activity in the pulmonary surfactant system, Chem. Phys. Lipids 141 (2006) 105–118.
[32] M.R. Morrow, J. Perez-Gil, G. Simatos, C. Boland, J. Stewart, D. Absolom, V. Sarin, K.M. Keough, Pulmonary surfactant-associated protein SP-B has little effect on acyl chains in dipalmitoylphosphatidylcholine dispersions, Biochemistry 32 (1993) 4397–4402.
[33] M.A. Oosterlaken-Dijksterhuis, H.P. Haagsman, L.M. van Golde, R.A. Demel, Characterization of lipid insertion into monomolecular layers mediated by lung surfactant proteins SP-B and SP-C, Biochemistry 30 (1991) 10965–10971.
[34] G. Vandenbussche, A. Clercx, M. Clercx, T. Curstedt, J. Johansson, H. Jornvall, J.M. Ruysschaert, Secondary structure and orientation of the surfactant protein SP-B in a lipid environment. A Fourier transform infrared spectroscopy study, Biochemistry 31 (1992) 9169–9176.
[35] J. Pérez-Gil, C. Casals, D. Marsh, Interactions of hydrophobic lung surfactant proteins SP-B and SP-C with dipalmitoylphosphatidylcholine and dipalmitoylphosphatidylglycerol bilayers studied by electron spin resonance spectroscopy, Biochemistry 34 (1995) 3964–3971.
[36] A.S. Dico, J. Hancock, M.R. Morrow, J. Stewart, S. Harris, K.M. Keough, Pulmonary surfactant protein SP-B interacts similarly with dipalmitoylphosphatidylglycerol and dipalmitoylphosphatidylcholine in phosphatidylcholine/phosphatidylglycerol mixtures, Biochemistry 36 (1997) 4172–4177.
[37] K. Shiffer, S. Hawgood, H.P. Haagsman, B. Benson, J.A. Clements, J. Goerke, Lung surfactant proteins, SP-B and SP-C, alter the thermodynamic properties of phospholipids membranes: a differential calorimetry study, Biochemistry 32 (1993) 590–597.
[38] A. Cruz, C. Casals, I. Plasencia, D. Marsh, J. Pérez-Gil, Depth profiles of pulmonary surfactant protein B in phosphatidylcholine bilayers, studied by fluorescence and electron spin resonance spectroscopy, Biochemistry 37 (1998) 9488–9496.
[39] A. Cruz, D. Marsh, J. Perez-Gil, Rotational dynamics of spin-labelled surfactant-associated proteins SP-B and SP-C in dipalmitoylphosphatidylcholine and dipalmitoylphosphatidylglycerol bilayers, Biochim. Biophys. Acta 1415 (1998) 125–134.
[40] D. Breitenstein, J.J. Batenburg, B. Hagenhoff, H.J. Galla, Lipid specificity of surfactant protein B studied by time-of-flight secondary ion mass spectrometry, Biophys. J. 91 (2006) 1347–1356.
[41] M. Seifert, D. Breitenstein, U. Klenz, M.C. Meyer, H.J. Galla, Solubility versus electrostatics: what determines lipid/protein interaction in lung surfactant, Biophys. J. 93 (2007) 1192–1203.
[42] J. Pérez-Gil, Comment to the Editor: properly interpreting lipid–protein specificities in pulmonary surfactant, Biophys. J. 94 (2008) 1542–1543.
[43] A.G. Serrano, M. Ryan, T.E. Weaver, J. Perez-Gil, Critical structure–function determinants within the N-terminal region of pulmonary surfactant protein SP-B, Biophys. J. 90 (2006) 238–249.
[44] I. Plasencia, A. Cruz, C. Casals, J. Perez-Gil, Superficial disposition of the N-terminal region of the surfactant protein SP-C and the absence of specific SP-B–SP-C interactions in phospholipid bilayers, Biochem. J. 359 (2001) 651–659.
[45] L.M. Loura, M. Prieto, F. Fernandes, Quantification of protein–lipid selectivity using FRET, Eur. Biophys. J. 39 (2010) 565–578.
[46] J. Bernardino de la Serna, J. Perez-Gil, A.C. Simonsen, L.A. Bagatolli, Cholesterol rules: direct observation of the coexistence of two fluid phases in native pulmonary surfactant membranes at physiological temperatures, J. Biol. Chem. 279 (2004) 40715–40722.
[47] G. Rouser, A.N. Siakotos, S. Fleischer, Quantitative analysis of phospholipids by thin-layer chromatography and phosphorus analysis of spots, Lipids 1 (1966) 85–86.
[48] L.M. Loura, A. Fedorov, M. Prieto, Partition of membrane probes in a gel/fluid two-component lipid system: a fluorescence resonance energy transfer study, Biochim. Biophys. Acta 1467 (2000) 101–112.
[49] D. Marquardt, An algorithm for least-squares estimation of non-linear parameters, J. Soc. Ind. Appl. Math (SIAM. J) 11 (1963) 431–441.
[50] V.E. Ahn, P. Leyko, J.R. Alattia, L. Chen, G.G. Prive, Crystal structures of saposins A and C, Protein Sci. 15 (2006) 1849–1857.
[51] A. Sali, T.L. Blundell, Comparative protein modelling by satisfaction of spatial restraints, J. Mol. Biol. 234 (1993) 779–815.
[52] K. Shiffer, S. Hawgood, H.P. Haagsman, B. Benson, J.A. Clements, J. Goerke, Lung surfactant proteins, SP-B and SP-C, alter the thermodynamic properties of phospholipid membranes: a differential calorimetry study, Biochemistry 32 (1993) 590–597.
[53] F. Fernandes, L.M. Loura, R. Koehorst, R.B. Spruijt, M.A. Hemminga, A. Fedorov, M. Prieto, Quantification of protein–lipid selectivity using FRET: application to the M13 major coat protein, Biophys. J. 87 (2004) 344–352.
[54] L.M. Loura, J.P. Ramalho, Location and dynamics of acyl chain NBD-labeled phosphatidylcholine (NBD-PC) in DPPC bilayers. A molecular dynamics and time-resolved fluorescence anisotropy study, Biochim. Biophys. Acta 1768 (2007) 467–478.
[55] A. Chattopadhyay, E. London, Parallax method for direct measurement of membrane penetration depth utilizing fluorescence quenching by spin-labeled phospholipids, Biochemistry 26 (1987) 39–45.
[56] J.E. Baatz, B. Elledge, J.A. Whitsett, Surfactant protein SP-B induces ordering at the surface of model membrane bilayers, Biochemistry 29 (1990) 6714–6720.
[57] A. Cruz, C. Casals, K.M. Keough, J. Perez-Gil, Different modes of interaction of pulmonary surfactant protein SP-B in phosphatidylcholine bilayers, Biochem. J. 327 (1997) 133–138.
[58] J.A. Killian, G. von Heijne, How proteins adapt to a membrane–water interface, Trends Biochem. Sci. 25 (2000) 429–434.
[59] A.G. Serrano, E.J. Cabre, J. Perez-Gil, Identification of a segment in the precursor of pulmonary surfactant protein SP-B, potentially involved in pH-dependent membrane assembly of the protein, Biochim. Biophys. Acta 1768 (2007) 1059–1069.
[60] S. Hawgood, M. Derrick, F. Poulain, Structure and properties of surfactant protein B, Biochim. Biophys. Acta 1408 (1998) 150–160.
[61] S. Krol, M. Ross, M. Sieber, S. Kunneke, H.J. Galla, A. Janshoff, Formation of three-dimensional protein–lipid aggregates in monolayer films induced by surfactant protein B, Biophys. J. 79 (2000) 904–918.
[62] John E. Baatz, D.R. Absolom, C. Baxter, J.A. Whitsett, Effects of surfactant-associated protein SP-B synthetic analogs on the structure and surface activity of model membrane bilayers, Chem. Phys. Lipids 60 (1991) 163–178.
[63] M.L. Longo, A.M. Bisagno, J.A. Zasadzinski, R. Bruni, A.J. Waring, A function of lung surfactant protein SP-B, Science 261 (1993) 453–456.
[64] C.Z. Wang, R.E. Barrow, C.S. Cox Jr., S.F. Yang, D.N. Herndon, Influence of detergent aerosol on lung microvascular permeability, J. Appl. Physiol. 74 (1993) 1016–1023.

[65] E. Parra, L. Hernandez-Moleiro, I. Lopez-Montero, A. Cruz, F. Monroy, J. Perez-Gil, A combined action of pulmonary surfactant proteins SP-B and SP-C modulate permeability and dynamics of phospholipid membranes, Biochem. J. 438 (2011) 555–563.
[66] B. Olmeda, L. Villen, A. Cruz, G. Orellana, J. Perez-Gil, Pulmonary surfactant layers accelerate O_2 diffusion through the air–water interface, Biochim. Biophys. Acta 1798 (2010) 1281–1284.
[67] E.J. Cabre, J. Malmstrom, D. Sutherland, J. Perez-Gil, D.E. Otzen, Surfactant protein SP-B strongly modifies surface collapse of phospholipid vesicles: insights from a quartz crystal microbalance with dissipation, Biophys. J. 97 (2009) 768–776.
[68] P.K. Wolber, B.S. Hudson, An analytic solution to the Forster energy transfer problem in two dimensions, Biophys. J. 28 (1979) 197–210.
[69] L. Davenport, R.E. Dale, R.H. Bisby, R.B. Cundall, Transverse location of the fluorescent probe 1,6-diphenyl-1,3,5-hexatriene in model lipid bilayer membrane systems by resonance excitation energy transfer, Biochemistry 24 (1985) 4097–4108.